A study of the ionospheric effect on GBAS (Ground-Based Augmentation System) using the nation-wide GPS network data in Japan

Takayuki Yoshihara, *Electronic Navigation Research Institute (ENRI)*
Naoki Fujii, *ENRI*
Akinori Saito, *Graduate School of Science, Kyoto University*

BIOGRAPHY

Takayuki Yoshihara is a researcher at ENRI, IAI. He received a Ph.D. in GPS application for meteorology from Kyoto University, 2001. His research interests are ionospheric and tropospheric effect on propagation delay of GPS signals. His research currently includes evaluation of atmospheric error on GBAS, and GPS down-looking occultation observation using aircraft. He is a member of IEICE and JIN.

Naoki Fujii is the leader of Ground Based Augmentation System (GBAS) research group and a Principle Researcher of Electronic Navigation Research Institute (ENRI). He was charged with development of the siting criteria of Instrument Landing System (ILS), Microwave Landing System (MLS) and Aircraft Address Monitoring System (AAMS) in ENRI. He is currently working in field of the development of Ground-Based Augmentation Systems for GNSS.

Akinori Saito, Ph. D., is a research associate of Department of Geophysics, Graduate School of Science, Kyoto University. He has studied the middle and low latitude ionosphere using data from GPS, radars, optical cameras, satellites and rockets. Since 1997, he and his colleagues have analyzed the ionospheric delay of GPS radio waves detected by GEONET in Japan.

ABSTRACT

This paper presents an investigation of spatial gradient of ionospheric delay that has a possibility of affecting GBAS (Ground-Based Augmentation System) using the nation-wide and dense GPS network in Japan (GEONET; GPS earth observation network). GBAS is a system based on a differential GPS technique for aircraft precision approach near an airport using C/A pseudorange. In general, ionospheric delay will be removable using correction data set that is generating and transmitting from a ground segment of GBAS. However, a large spatial gradient of ionospheric delay between ground GPS monitoring station and aircraft will be a risk to integrity of GBAS. Therefore, our purpose is to exactly estimate local-scale variation of ionospheric delay.

Because Japan is located in lower geomagnetic latitude than geographic latitude, 'Equatorial anomaly' phenomenon is especially remarkable for generating a variation of ionospheric delay gradient in the North-South direction. GEONET is consists of about 1,000 GPS stations using dual-frequency receiver and a typical distance between neighbor stations is about 20 km. We used Total Electron Content (TEC) data of GEONET with a correction of inter-frequency bias that provided from TEC database of Kyoto University, Japan.

Firstly, we investigated general characteristic of spatial gradient of ionospheric delay over Japan using TEC data with rough grid and time resolutions. In distribution analysis of the number of times for each magnitude of gradient in the S-N direction, the results were consistent with the matter that growth of equatorial anomaly produced large TEC gradient toward south.

Secondly, in order to detect smaller perturbation of spatial gradients, we used 'grid TEC' of TEC database, which sorted from each pierce point into each grid with a spatial resolution of 0.15 degree in longitude and latitude. We calculated and investigated spatial gradient after averaging TEC with a spatial resolution of 1-degree-grid and a time resolution of 15 minutes at the point with the maximum slant path density. The results were consistent with our expectation that small-scale perturbations were correctly represented.

Finally, we investigated local spatial gradient of ionospheric delay for the both of the N-S and the E-W direction using one-year-data-set of co-located 4 stations within several 10 km along the N-S and the E-W direction, respectively. As a result, we recognized that spatial gradients were increased in spring and autumn, when TEC variations were large, and were larger in the case of the N-S direction than the E-W one. We concluded that ionospheric slant delay data of TEC database is very useful for a study of local spatial gradient.

INTRODUCTION

GBAS is a system based on a differential GPS technique for aircraft precision approach near an airport. Therefore, ionospheric and tropospheric delay can be almost removed using GBAS. However, it was pointed out that a large spatial gradient in ionospheric delay often produces a significant positioning error on GBAS through the carrier smoothing method [1]. In GBAS, reference station on the ground provides correction data of C/A code pseudorange, which contains receiver noise, the ionospheric and the tropospheric delays, and transmits them to aircraft together with an evaluation parameter for the each error source. The aircraft segment of GBAS receives them and calculates aircraft position with a protection level (PL), which evaluates a reliability of a final positioning solution, in real time.

Electronic Navigation Research Institute (ENRI), Japan has been developing and evaluating GBAS by performing flight experiments in Sendai airport, Japan [2]. If a larger value than a real variation is selected for an evaluation parameter in order to maintain a reliability of solution, underestimation of availability for GBAS will be caused. Therefore, we aim to exactly estimate evaluation parameter for each error source in GBAS correction data, especially, on ionospheric variation in Japan.

Because Japan is located in lower geomagnetic latitude than geographic latitude, there are various ionospheric phenomena. The equatorial anomaly is a phenomenon that is characterized in spatial distribution with the maximum of electron density at the both of geomagnetic latitude of 15 N and 15 S. Therefore, it produces a spatial gradient of ionospheric delay on GPS signal along the N-S direction over Japan. As a result, a spatial gradient along the N-S direction is directly affected by its activity. In the Southern area in Japan, 'plasma bubble' is often occurred. It is an ionospheric phenomenon with a horizontal scale of about 100 km in the E-W direction and several 1,000 km in the N-S direction, respectively. It produces significantly scintillation on GPS signal and time variation of ionospheric delay.

Although various ionospheric phenomena produced the both of spatial and time gradients of propagation delay on GPS signal, we especially investigated spatial gradient in this paper. We calculated spatial gradient for the both directions from South to North (the S-N direction) and from West to East (the W-E direction) using GEONET / TEC database of Kyoto University with a correction of inter frequency bias. Firstly, nation-wide characteristic of spatial gradient of ionospheric delay over Japan was investigated using TEC data with a rough grid and a temporal resolution. Secondly, we aimed to investigate small variation of spatial gradient that was calculated using slant TEC after averaging with a spatial resolution of 1-degree-grid and a time resolution of 15 minutes. Finally, we investigated local spatial gradient in the N-S and the W-E direction using 4 stations co-located within several 10 km along the E-W and the N-S direction, respectively. Note that we used ionospheric data in 2001.

TEC DATABASE USING GEONET

The Geographical Survey Institute (GSI) of Japan has arranged and been operating about over the 1,000 GPS dual-frequency receivers all over Japan, which is called by GEONET (GPS earth observation network). Although the primary purposes of GEONET are monitoring and detecting seismic deformation, it is useful for various geophysical observations, i.e. Precipitable water vapor (PWV) estimated from tropospheric delay, Total Electro Content (TEC) from dual-frequency observation, etc. In December of 2001, 983 stations were available. A corresponding distance between two stations was about 20 km.

Because of the inter-frequency bias problem, we cannot directly estimate spatial gradient from GEONET observational data. Therefore, we have to estimate inter-frequency bias from raw data. Solar-Planetary Electromagnetism Laboratory (SPEL) of Kyoto University, Japan has estimated inter-frequency bias for GEONET stations to obtain slant TEC and has stored them as 'TEC database'. In this paper, we used TEC data that was provided from TEC database to calculate spatial gradient of ionospheric delay.

The details of processing of TEC database to estimate inter-frequency bias are described in [3]. We briefly introduce the summarized processing. The slant TEC were calculated by the following strategies under the assumptions that the inter-frequency bias was constant during each day and that ionosphere feature is thin shell model with a height of 400 km. The cut off elevation angle is 30 degrees. Note that they estimated inter-frequency bias for each pair of one satellite and one station.

1. At first, they estimate the inter-frequency bias for each satellite-station pair under the assumptions of homogeneous ionosphere within coverage area by a receiver and of a constant vertical TEC in during one hour. They also calculate 'hourly TEC' with a spatial resolution of 2 degrees in the longitude and the latitude using TEC results of all stations.

2. With a little adjustment for each inter-frequency bias using hourly TEC results, TEC along each slant path ('slant TEC') is estimated for each pair of a satellite and a station.

3. A vertical TEC is calculated from each slant TEC and mapped on ionospheric shell with a pixel of 0.15 x 0.15 degree in the geographic longitude and latitude (called by 'grid data'). They also provide 'slant TEC' data set that is sorted into each station.

Note that TEC, ionospheric delay and spatial gradient are projected in the zenith direction and that delay is represented in effect on L1-band in this paper.

NATION-WIDE ANALYSIS

At first, we used TEC data with a spatial resolution of 2-degree-grid and a time resolution of 1-hour to investigate gradient variations with nation wide scale of Japan. This data set is called as 'hourly TEC', which was estimated together with inter-frequency bias. Figure 1 shows the number of each grid on DOY (Day of Year) of 001. The feature of the data distribution is long in the North-South direction because of the GEONET sites distribution on the ground. To investigate dependence of ionospheric delay gradients on latitude, we selected three points, which are A (41 N, 141 E), B (37 N, 137 E) and C (33 N, 133 E).

For example, we show ionospheric vertical delay during 2001 at the point of B in Figure 2. Note that the time is represented in UT (Japanese local time is 9 hours early from UT). We defined 4 seasons, which were winter (DOY of 001 - 046), spring (047-137), summer (138-228) and autumn (229-319), to investigate seasonal variations of spatial gradient.

Because Japan is located in lower geomagnetic latitude than geographic latitude, there is an ionospheric phenomenon of the equatorial anomaly, which produces large variation of TEC spatial distribution along the N-S direction. Therefore, we calculated spatial gradient of ionospheric delay (mm/km) on L1-band in the S-N direction. Note that each spatial gradient was calculated using TEC at three grids.
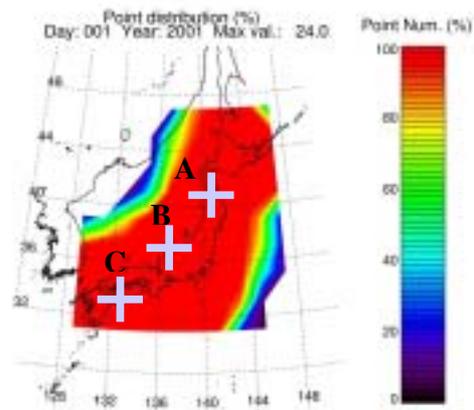

Figure 1: The data number of each grid (2 x 2 degrees) on DOY (day of year) of 001. The maximum was 24 data because of time interval of 1-hour. Colors indicate ratio to maximum number.
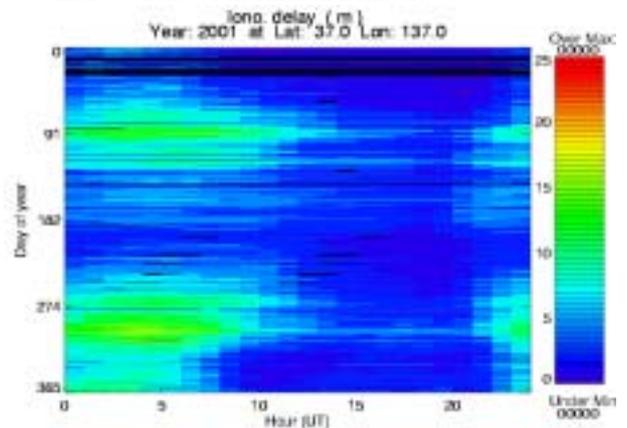

Figure 2: Ionospheric L1-delay at the point of 'B' of Figure 1 in 2001. Ionospheric delay was calculated form 2-degree-grid TEC data. A black point indicates loss of data.

The results for gradient in the S-N direction at the point of B are shown in Figure 3 and Figure 4. Seasonal averaging gradients in the S-N direction were generally in negative as actual ionosphere. The absolute maximum of seasonal averaged gradient was daytime in autumn as shown in Figure 4. In summer, spatial gradient of ionospheric delay was small during daytime and nighttime.

We investigated the number of times divided for each magnitude with an interval of 0.08 mm/km of ionospheric delay gradient in the S-N direction for each season as shown in Figure 5. In the figure, it was also represented the results of Gaussian curve fitting. Since absolute TEC was generally higher in the south side, the center of Gaussian distribution was in negative. The deviation from Gaussian distribution curve was large toward negative especially in autumn. These results are consistent with the matter that growth of equatorial anomaly produces large TEC gradient toward south, i.e. large negative gradient in

the S-N direction. In summer, because of small TEC variation, the deviation from Gaussian distribution curve was small.
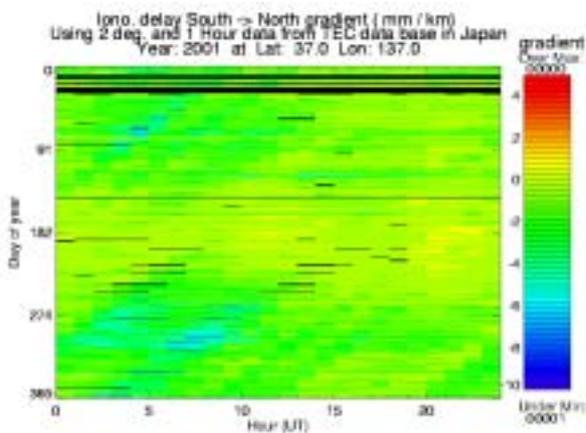

Figure 3: Spatial gradient of ionospheric delay in the S-N direction at the point of B in 2001. The results are plotted by DOY-Hour section. A black point indicates loss of data.
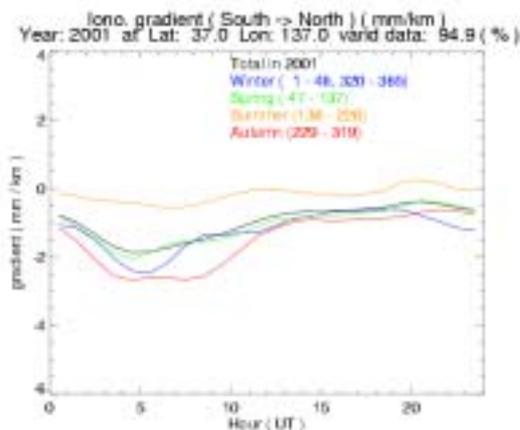

Figure 4: Spatial gradient of ionospheric delay in the S-N direction that was averaged for each season at the point of 'B' (37 N, 137 E). Black line shows result that was averaged during total year of 2001.

The same analysis was performed at the points of A and C of Figure 1 in order to investigate dependence of gradient in the S-N direction on latitude. As a result, we recognized that the characteristics of seasonal variation at the both A and C points ware similar to the point of B. Here, we show the same results as Figure 5 except for at the points of A and C only in autumn in Figure 6.
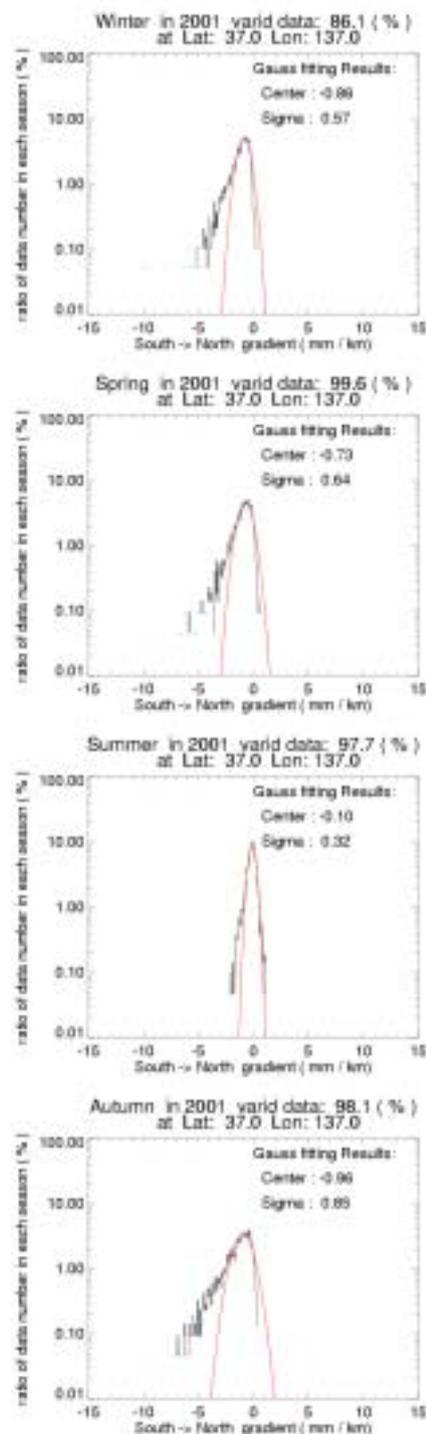

Figure 5: The number of times divided for each magnitude with an interval of 0.08 mm/km in ionospheric delay gradient in the S-N direction at the point 'B' (37 N, 137 E). Each figure from the Top to Bottom indicates the result for winter, spring, summer and autumn, respectively. Note that the data number was represented in ratio to total numbers of each season and plotted with a log scale. Red lines represent results of Gaussian curve fitting.
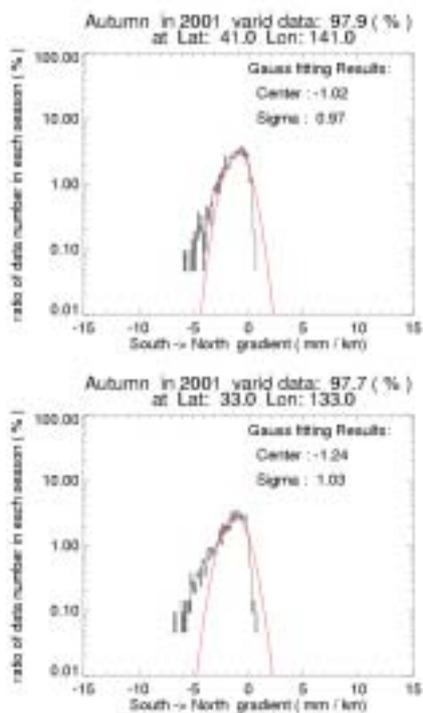
Figure 6: The same as Figure 5 except the results in autumn and at the point 'A' (41 N, 141 E) and 'C'. (33 N, 133 E). The top and the bottom ware the result of A and C, respectively.

The characteristics of the center of Gaussian distribution and of deviation from Gaussian curve ware similar each other at the point A and C, except slightly larger at the point of C, which was at lower latitude than the point of A. Because the activity range of equatorial anomaly is up to about 40 N, it is expected that the distribution of the number of times divided for each magnitude is similar to Gaussian curve in the more Northern area.

Additionally, we investigated the ionospheric gradient in the W-E direction. We recognized that the seasonal variation in sigma of Gaussian curve was characterized that the maximum was in autumn and that the minimum was in summer as the same as the results in the S-N direction. Therefore, we show the results only in autumn. Figure 7 shows spatial gradient in the W-E direction at the point A, B and C in autumn. Note that we corrected gradient in the W-E direction so that seasonal averaging result may be 0. In this figure, the width of Gaussian curve was wider in the lower latitude. Because absolute TEC was larger in the lower latitude, it seemed that daily variation was represented on gradient in the W-E direction.
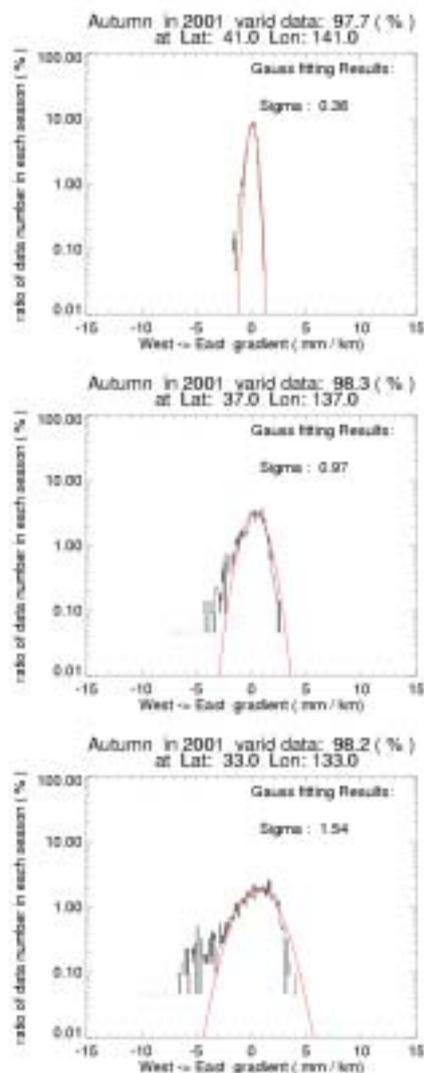

Figure 7: The same as Figure 6 except that the W-E spatial gradient at the point 'A' (41 N, 141 E), 'B' (37 N, 137 E) and 'C' (33 N, 133 E) in autumn were plotted from the Top to Bottom, respectively. Note that we corrected the W-E gradient so that seasonal averaging result may be 0.

MIDDLE-SCALE ANALYSIS

Secondly, we used vertical 'grid TEC' in TEC database, which was calculated for each pair of one satellite and one station (i.e. Slant TEC with a projection to the zenith) with an original sampling time of 30 seconds. It was also mapped on ionospheric shell at each pierce point and sorted into a pixel of 0.15 x 0.15 degree in longitude and latitude. Because of configurations of GPS satellites and ground stations, there was not enough data number to calculate gradients with an original grid size and time resolution with maintaining time and spatial continuities. Therefore, we have to perform temporal and spatial

integration. In Figure 8, the path density after daily averaging was plotted with a time interval of 15 minutes and a spatial resolution of 1-degree-grid in longitude and latitude. The configuration of path density is the almost same every day except a time lag of about -4 minutes. In the Northern and the Southern area, path densities were smaller than the center of Japan Islands. The point with the maximum path density was calculated as the point of 36.5 N, 137.5 E. Therefore, we calculated spatial gradient at this point.
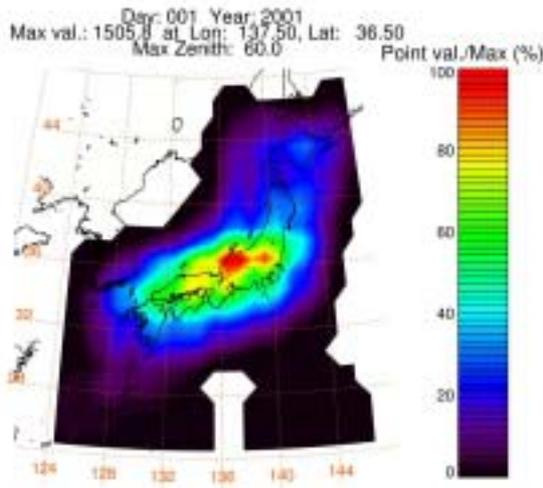
Figure 8: Path density of vertical 'grid data' using one-day-data-set. Note that path density was calculated with a spatial resolution of 1-degree grid and a time interval of 15minutes using vertical TEC data with a zenith angle of less than 60 degrees.

In the integration of vertical TEC with a spatial and temporal interval, we took in account of satellite distinction because each vertical TEC was a result along each ray path. Figure 9 shows error in determination of integrated TEC with a spatial resolution of 1-degree-grid and a time interval of 15 minutes using all satellites with a zenith angle of less than 60 degrees. A large error was occurred especially around the central of Japan, where path density was large. Therefore, we used one satellite for TEC integration within each grid and during each time interval. We define the best satellite as a satellite with a zenith angle of less than 30 degrees and of the minimum in each grid. Figure 10 shows the results with the best satellite analysis. Because the integrated TEC in each grid represented the results of one satellite, the error was reduced in comparison with Figure 9.

Using the TEC that was integrated from the best satellite for each grid and time interval, we calculated spatial gradient in the S-N direction. Note that we calculated gradient from the same-satellite-integrated TEC at three grids. Therefore, in the case such as that different satellite was selected at neighbor grids, we regarded as loss of data.

We additionally regarded an integrated TEC with a R.M.S of more than 30 % as an abnormal datum and did not use it.
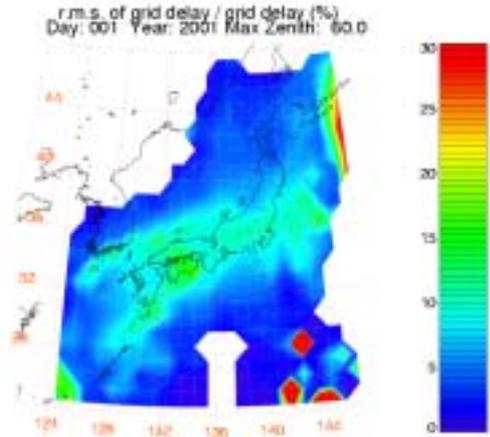

Figure 9: R.M.S of differences between integrated ionospheric delay within 1-degree-grid and with a time interval of 15 minutes using vertical TEC of all satellite with a zenith angle of less than 60 degrees on DOY of 001, 2001. Note that a R.M.S is normalized with absolute of each integrated TEC (in %).
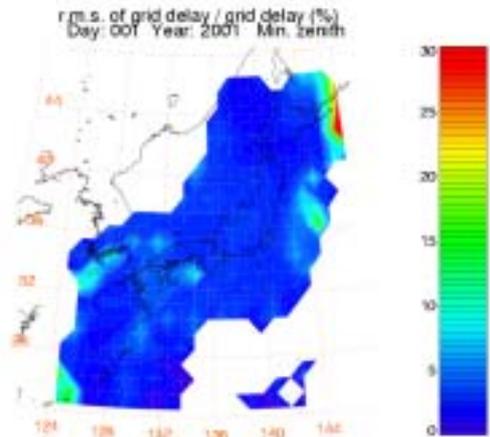

Figure 10: The same as Figure 9 except using one satellite with a zenith angle of less than 30 degrees and of the minimum in each grid and time interval.

Figure 11 shows spatial gradient of ionospheric delay in the S-N direction with a spatial resolution of 1-degree-grid in longitude and latitude and with a time interval of 15 minutes in 2001. It seems that smaller perturbations were represented than the results with a spatial resolution of 2-degree-grid and a time resolution of 1-hour. Seasonal

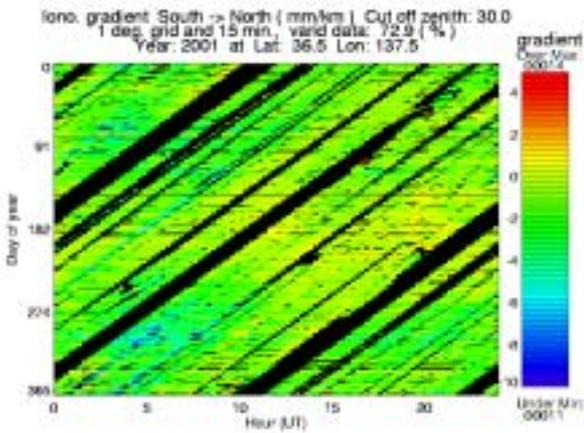averaging gradient in the S-N direction were generally in negative (shown in Figure 12).

Figure 11: Spatial gradient of ionospheric delay in the S-N direction with a spatial resolution of 1-degree-grid in longitude and latitude and with a time interval of 15 minutes in 2001. Note that the results at the point with the maximum path density (36.5 N, 137.5 E) were plotted. A black point indicates loss of data with the satellite selection.
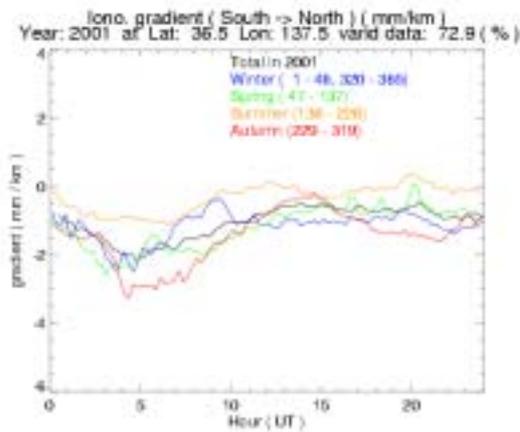

Figure 12: Spatial gradient of ionospheric delay in the S-N direction that were averaged for each season at the point with the maximum path density (36.5 N, 137.5 E).

We investigated the number of times divided for each magnitude with an interval of 0.08 mm/km in the S-N gradient as the same analysis with 2-degree-grid. Figure 13 shows gradient in the S-N direction using TEC with 1-degree-grid in the both longitude and latitude at the point with the maximum path density (36.5 N, 137.5 E). As same as the results in 2-degree-grid analysis, the center of Gaussian distribution was in negative every season.

Moreover, large negative deviations from Gaussian fitting curve were more occurred, even in summer. It seemed that the variation within a horizontal scale of less than 2 degrees and a temporal scale of less than 1-hour were represented in Figure 13.
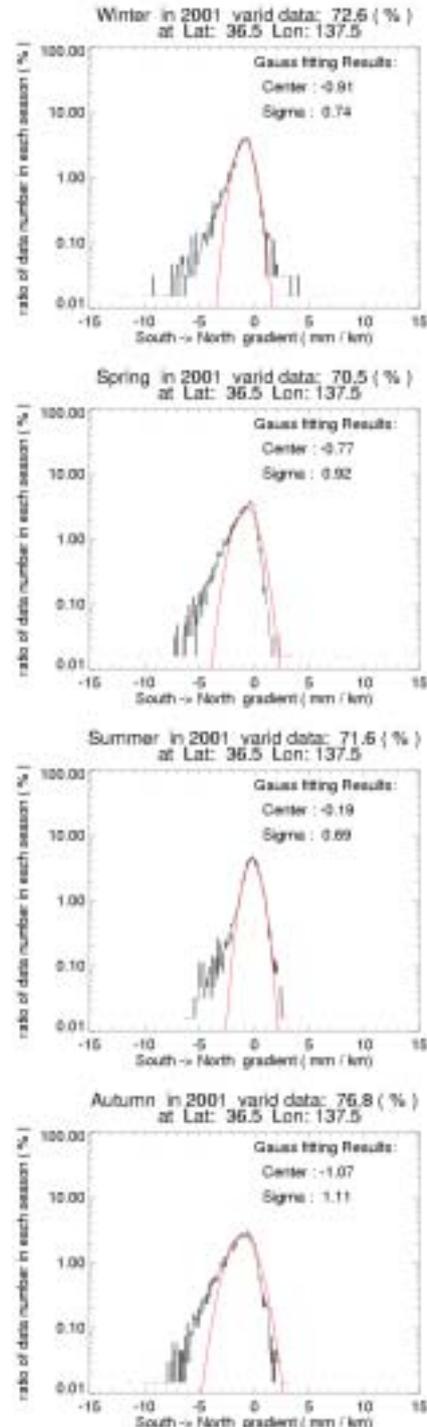

Figure 13: The same as Figure 5 except for gradient in the S-N direction using TEC data with 1-degree-grid in the both longitude and latitude at the point with the maximum path density (36.5 N, 137.5 E).
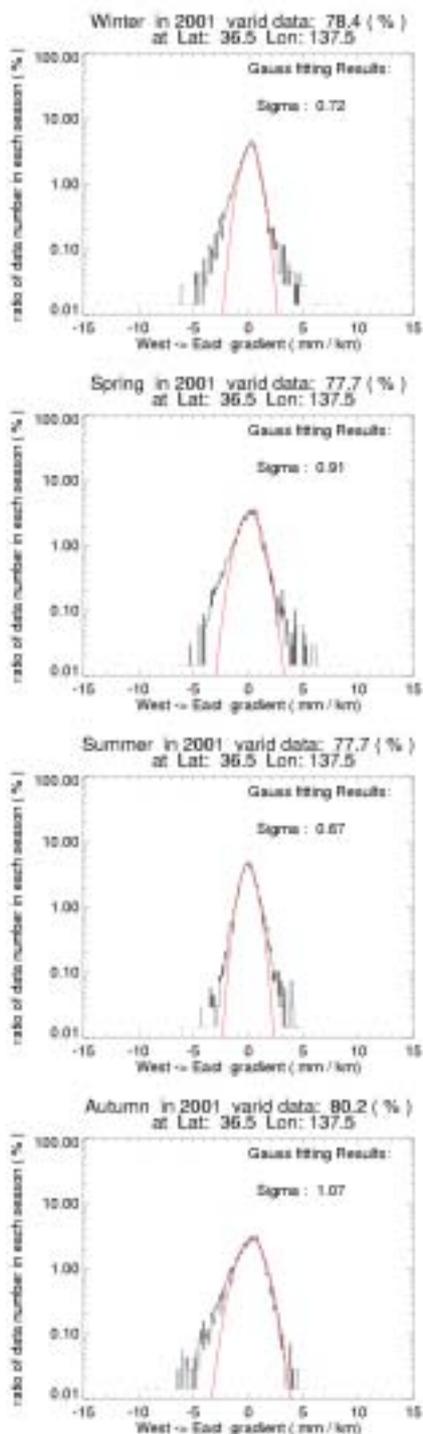
Figure 14: The same as Figure 13 except for plotting of the W-E gradient. Note that we corrected the W-E gradient so that each seasonal averaging result may be 0.

We also show results of gradient in the W-E direction. Note that we corrected gradient in the W-E direction so that each seasonal averaging result may be 0 as the same as 2-degree-grid analysis. Figure 14 shows the number of

times divided for each magnitude of 0.08 mm/km. The result of Gaussian curve fitting was over plotted. In comparison with the W-E gradient in analysis using 2-degree-grid, deviation from Gauss curve was a more symmetrical form. Because of contributing of daily variation in the W-E gradient, this results ware consistent with the previous consideration that small perturbation of ionospheric delay gradient were detected.

We could analyze spatial gradient with a good spatial and temporal resolution around the area with the maximum path density. However, path density was reduced in the lower and higher area on account of station distributions. Consequently, available data number is reduced by data selection algorism in this paper. An investigation of the other domains is a future subject.

LOCAL SCALE ANALYSIS

Finally, we used slant TEC data obtained at each station in the densest area of GEONET to investigate ionospheric gradient within several 10 km. We selected total of 7 stations located along the N-S and the E-W directions (shown in Figure 15). The same type receivers (Trimble 4000SSE) ware selected. Using 4 stations nearly aligned along each the N-S and the W-E direction, we calculated spatial gradient along the receivers' forming with a time averaging of 10 minutes. Note that the original sampling rate was 30 seconds. We also selected a cut-off zenith angle of 30 degrees and used slant TEC of one GPS satellite with the minimum zenith angle and in common view at 7 stations for each time interval. Namely, we used the same satellite. As same as in middle-scale analysis, the case that different satellites were selected as a satellite with the minimum zenith angle at neighbor stations, we regarded as loss of data.

Although we used the same satellite in local gradient analysis in each time interval, satellite will be change at the other period. Therefore, it is expected that results are combinations of TEC observed using various GPS satellites. Namely, because ionospheric delay gradient of each satellite represents condition along own slant path, the results depend on satellite configurations. We used the 1-year-data-set. The almost same satellite configuration repeated about 4-minute-earlier every day. Under the above condition, we calculated spatial gradient of ionospheric delay (mm/km) in the both directions of the S-N and the W-E using 4 stations along each direction. Note that gradient is represented in a projected value to vertical direction.

The number of times divided for each magnitude with an interval of 0.08 mm/km in the S-N and the W-E gradient were shown in Figure 16 and Figure 17, respectively. Note that we corrected the W-E gradient so that each

seasonal averaging result may be 0. From two figures, general characteristics were similar each other in the both directions. Namely, ionospheric gradient was small in summer, and was large in spring and autumn.

Because the results were combination of gradients using various GPS satellites with a rotation of about 24 hours, sigma values of Gaussian curve were large in the both directions. However, we also recognized that there were more data with a large deviation in the S-N than the W-E direction. In the other word, the deviation from Gaussian curve was larger in the S-N than the E-W direction. We could also recognize that the deviation from Gaussian curve was a more symmetrical form in the W-E gradient. The maximum of absolute gradient was observed as –26.8 mm/km in the S-N direction, and –31.6 mm/km in the E-W direction in spring.
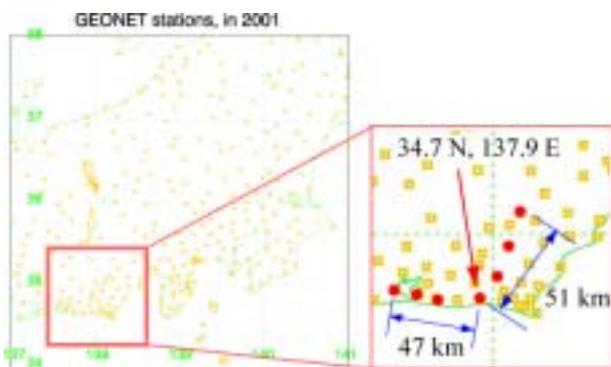

Figure 15: We selected total of 7 stations (Red circles), which could form nearly straight line along each direction in the S-N and the W-E by 4 stations of them, respectively.

SUMMARY

We investigated spatial gradient of ionospheric delay along the both directions from South to North and from West to East using 'TEC database' with the three scales in spatial and temporal resolution in Japan.

At first, we investigated characteristics of spatial gradient with a nation-wide scale using 2-degree-grid and 1-hour TEC data. The gradients at the three points of the Northern, the Central and the Southern of Japan were calculated and investigated through the analysis of the number of times divided for each magnitude. We recognized that a deviation from Gaussian fitting curve was large every site in the S-N gradient. Moreover, because of the equatorial anomaly, distribution curve was not similar to Gaussian curve except in summer. However, dependence of gradient in the S-N direction on latitude is not so large in contrast with the W-E gradient.

Secondly, to investigate smaller perturbation of spatial gradient than 2-degree-grid analysis, we used 1-degree-grid TEC data with a time resolution of 15 minutes. In calculations, we selected one GPS satellite with the minimum zenith angle and in common view of the neighbor grids during each time interval. From the same analysis using 2-degree-grid, the deviation from Gaussian curve was generally larger in comparison with the 2-degree-grid results. We also recognized that the deviation from Gaussian curve in the W-E gradient was a more symmetrical form. From these results, small perturbation of ionospheric delay, e.g. daily variation, was reflected in results.

Finally, we calculated local spatial gradient using total of 7 stations in the densest area of GEONET. We also used a common satellite in 7 stations during each time interval. Because the results were combination of gradients using various GPS satellites with a rotation time of about 24 hours, sigma value of Gaussian curve was large in the both directions. We also recognized that a large negative gradient in the S-N direction was occurred more times than the W-E direction.

Ionospheric slant delay data of TEC database is very useful for a study of local spatial gradient. Therefore, we are going to investigate the other area, especially in the Southern of Japan taking in account of spatial path density of GEONET.

REFERENCES

[1] Jock R. I. Christie, P. Ko, B. Pervan, P. Enge, J. Powell, B. Parkinson, "Analytical and Experimental Observations of Ionospheric and Tropospheric Decorrelation Effects for Differential Satellite Navigation during Precision Approach", *ION GPS*, Sep, 1998

[2] S. Saitoh, S. Fukushima, T. Yoshihara and N. Fujii; "Experimental GBAS Performance at the Approach Phase", *Proceedings of the ION NTM 2003*, pp 317-325, Jan., 2003

[3] Y. Otsuka, T. Ogawa, A. Saito, T. Tsugawa, S. Fukao, and S. MIyazaki, *Earth Planets and Space*, 54, pp 63-70, 2002
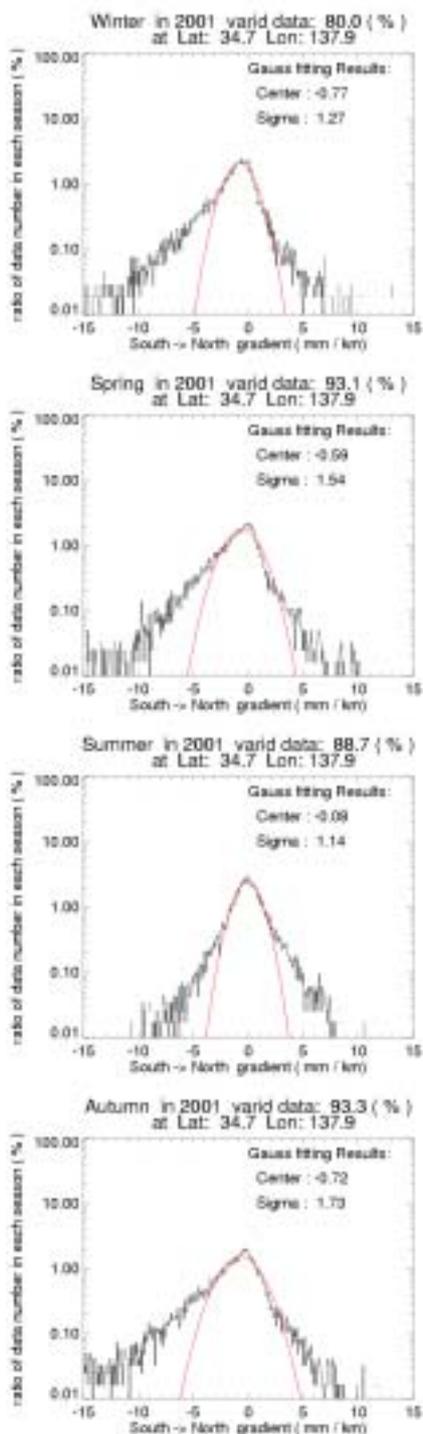
Figure 16: The number of times divided for each magnitude with an interval of 0.08 mm/km in the S-N gradient using the 4 stations (34.7 N, 137.9 E). Each figure from the Top to Bottom indicates the results for winter, spring, summer and autumn, respectively. Note that the data number was represented in ratio to total numbers of each season with a log scale. Red lines represent results of Gaussian curve fitting.
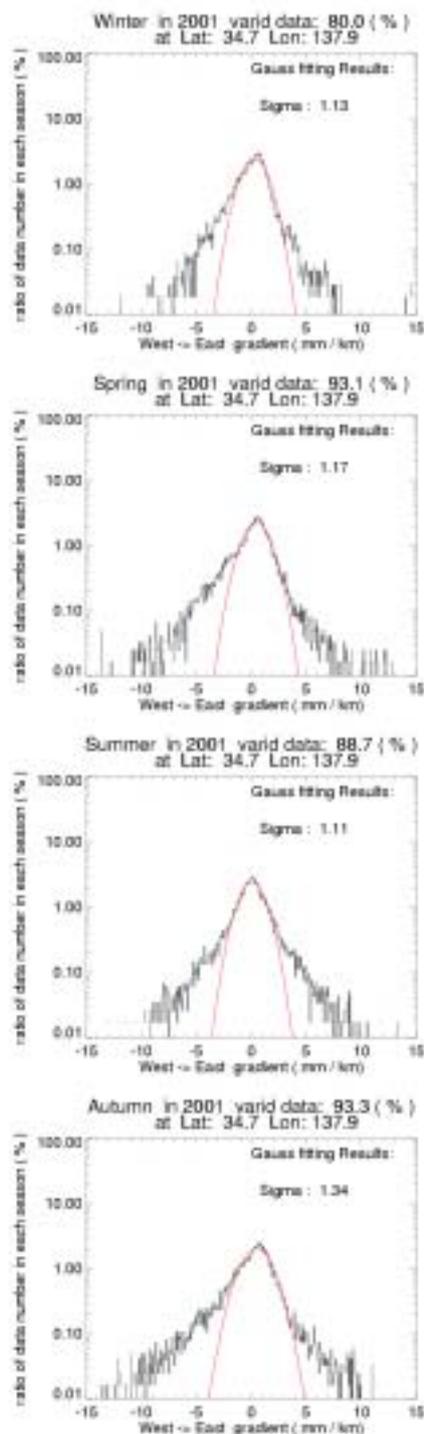
Figure 17: The same as Figure 16 except for plotting of the W-E gradient. Note that we corrected the W-E gradient so that each seasonal averaging result may be 0.